

Local Arterial Input Functions based on Vascular Territories

S. Christensen¹, O. Wu^{1,2}, N. Hjort¹, K. Mouridsen¹, C. Gottrup¹, J. Fiehler³, J. Röther³, L. Østergaard¹

¹CFIN, Dept. of Neuroradiology, Århus University Hospital, Århus, Denmark, ²Image Sciences Institute, University Medical Center Utrecht, Utrecht, Netherlands, ³Dept. of Neuroradiology, Hamburg-Eppendorf, Hamburg, Germany

Introduction

Calculation of CBF using Perfusion-weighted MRI requires deconvolution of the tissue concentration time curve (TC) by the arterial input function (AIF) on a voxel by voxel basis [1, 2]. It is common practice to select one AIF from a major artery and use that AIF for the deconvolution of all image TCs. The SVD deconvolution technique commonly used is, however, sensitive to time delays between the AIF and the TCs as well as to dispersion of the AIF distal to the site of selection [1, 3, 4]. In normal subjects, this may affect CBF estimates due to differences between the anterior and posterior circulations, and in acute stroke, where arterial blood reaches the tissue by collaterals, residual perfusion may be underestimated. Ideally, the AIF used for the deconvolution should hence apply to the tissue being analyzed, rather than being a single global AIF. Attempts to improve this shortcoming include the delay insensitive circular SVD [5] and the local AIF method presented by Alsop et al. [6]. Where the first technique does not account for dispersion, the latter has inherent difficulties in consistent AIF selection criteria across vascular territories. In this study we present a method that allows selection of AIFs for each of the six major vascular territories hence accounting for delay and dispersion.

Materials and Methods

A three-dimensional map outlining major vascular territories was superimposed on the MNI305 average brain in order to locate it in a stereotaxic coordinate system [7-9].

Individual patient data were then coregistered to the MNI305 brain using automated image coregistration tools from the MNI, resulting in a mask of vascular territories that mapped onto the patients raw EPI perfusion data [10]. A graphical user interface was built using Matlab® to enable the user to select AIF voxels within each of the vascular territories based on the appearance of the concentration time curve. See Figure 1 and 2. The border zones between segments were assigned a probability of belonging to a given segment based on the volume fractions of neighboring segments. These probability maps were then used to weigh the corresponding territory AIFs, resulting in smooth transitions across border zones between segments, see Figure 1. The smoothing (performed only between segments in the same hemisphere) mimics the dual/triple territory supply in territory border zones. With this AIF for each voxel, the TCs were then deconvolved with the AIFs on a voxel by voxel basis and flow is determined as the maximum height of the residue function. The deconvolution was implemented by using oscillation index regularized circular SVD (oSVD) [5]. This accommodates for the fact that even a local main segment AIF may differ from downstream subsegment AIFs in the same territory by a simple delay.

Acute stroke patients undergoing a protocol of acute DWI/PWI on a 1.5 T scanner (Siemens) (PWI by gradient echo EPI, TR/TE=1500/45.3 ms) within 6 hours of symptom onset (n=12) were retrospectively analyzed by the standard SVD algorithm (sSVD) [2], oSVD and the proposed local AIF method (lcAIF). The two former, global AIF techniques used the contralateral MCA territory AIF for deconvolution. The algorithm was tested for stability and MTT maps by the three techniques compared visually for systematic differences in terms of the visualization of perfusion abnormalities.

Results and Discussion

The method was stable and produced territorial AIFs that in most patients clearly indicate differences in AIF timing among the unaffected PCA, MCA and ACA territories (Figure 1). The AIF in the affected vascular territories displayed various degrees of delay and dispersion resulting in visible differences in the appearance of MTT maps. Notice on Figure 2 (47 yo patient) how the right MCA AIF (yellow curve) is more dispersed than the one selected contralaterally. Figure 3 shows the corresponding MTT maps. The sSVD shows prolonged MTT in most of the right MCA territory, possibly due to its sensitivity to the delays and dispersion of the AIF. The oSVD, mainly sensitive to dispersion but not the observed delay, tends to delineate a smaller area as having high MTT values, emphasizing how delayed bolus arrival negatively impacts flow estimates when using sSVD.

The lcAIF MTT maps show an area of abnormal MTT values that is slightly smaller than that produced by the oSVD global AIF method – especially in the uppermost slices. The lcAIF uses the dispersed bolus for deconvolution in that way avoiding MTT overestimation.

The method has the potential to visualize major vessel abnormalities by the timing of the arterial supply of their vascular territories (Figure 1). We speculate that the segmentation may stabilize automatic AIF detection algorithms such as the method proposed by Alsop et al. [6] to further account for intra-segment delay and dispersion, further improving flow estimates. Finally, the segmentation of the brain into vascular territories lends itself to introduce new risk estimates in predicting outcome, taking into account the vascular segment and spatial location herein (central/watershed) of CBF abnormality.

Conclusion

The method allows selection of territory specific local AIFs thereby minimizing the unwanted effects of delay and dispersion of the bolus previously shown to bias CBF and MTT estimates [1, 3-5]. The method will need further validation in terms of improving CBF estimates and delineation of tissue-at-risk in acute stroke.

References

- [1] L. Østergaard, et al., Magn Reson Med,36, 726-36, 1996. [2] L. Østergaard, et al., Magn Reson Med,36, 715-25, 1996. [3] O. Wu, et al., Magn Reson Med,50, 856-64, 2003. [4] F. Calamante, et al., Magn Reson Med,44, 466-73, 2000. [5] O. Wu, et al., Magn Reson Med,50, 164-74, 2003. [6] D. Alsop, et al., ISMRM Proceedings, 659, 2002. [7] S. A. Berman, et al., AJR Am J Roentgenol,135, 253-7, 1980. [8] L. A. Hayman, et al., AJR Am J Roentgenol,137, 13-9, 1981. [9] D. Collins, JCAT.,18, 192-205, 1994. [10] D. MacDonald, et al., "The MNI tools.",<http://www.bic.mni.mcgill.ca/software/>.

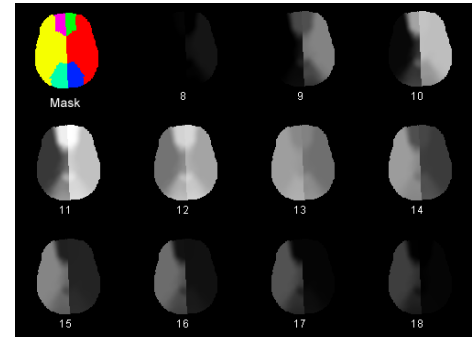


Figure 1 Territory mask and regional AIF

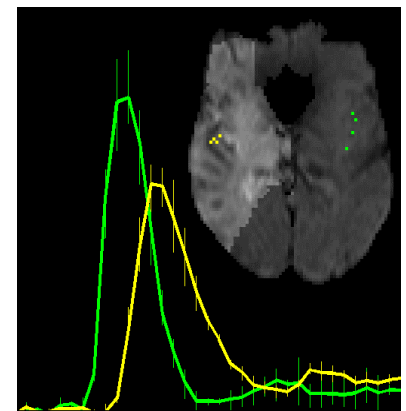


Figure 2 Highlighted part shows MCA territory. Note dispersion differences between hemispheres

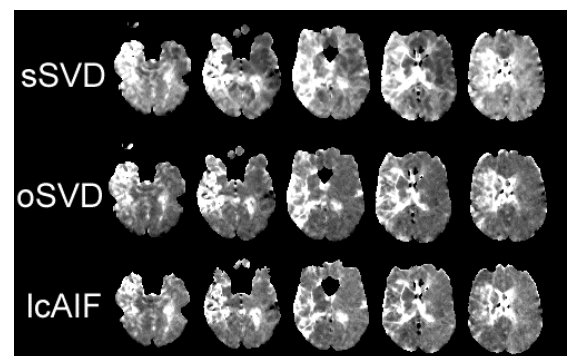


Figure 3: MTT maps for the 3 techniques